$(\eta^6C_6H_6)(\eta^5\text{-}C_5H_5)^+$ ions, $\phi_L$ values (313 nm excitation) are markedly medium-dependent, being significantly larger in more nucleophilic solvents. For Ib quantum yields were reduced even in the presence of relatively small concentrations of $CH_3CN$ in the aqueous solution.

In these contexts, a potential mechanism for this reaction would be for the excited state, having a distorted metal–arene bond, to undergo competitive deactivation to the ground state (or less reactive lower energy states) or reaction with solvent to give an intemediate species such as a solvated $\eta^4$-arene, e.g.

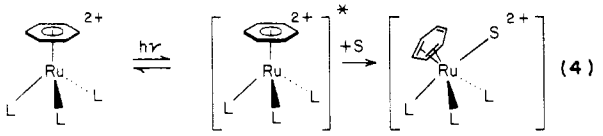


(4)

This intermediate would also have the option of reacting further to give the fully solvated product or to lose S to regenerate the starting complex, e.g.

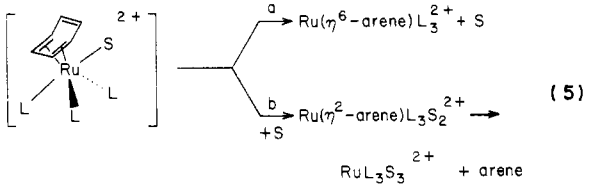


(5)

Analogous mechanisms have been proposed for the mechanisms for the thermal exchange of solution and coordinated arenes.[20]

The overall quantum yield for eq 4 would be determined by the branching efficiencies at each stage of this of this mechanism. More nucleophilic solvents would therefore be expected to favor arene labilization. Alkyl substitution perhaps would inhibit solvent attack in eq 4 owing to steric effects as well as make the arene a stronger nucleophile, better able to displace S from the $\eta^4$ intermediate. Both effects would lower the efficiency of photolabilization as observed. The $\Delta V^*$(apparent) measured for such a mechanism would reflect the volume differences between the transition states of competing pathways (e.g., eq 5a or 5b), leading to starting material or to product. The small value of this parameter suggests that the volume profile for steps leading back to starting material or going on to products involve comparable $\Delta V^*$ values. For eq 5a and 5b, this would be consistent with both such pathways being essentially interchange processes between ligands in the first and second coordiations spheres thus having $\Delta V^*$ values of the same sign and similar magnitudes (probably small).

**Acknowledgment.** This research was supported by National Science Foundation grants (INT83-04030 and CHE81-20266) to P.C.F. W.W. acknowledges NATO for a postdoctoral fellowship via the Deutscher Akademischer Austausch Dienst (DAAD).

**Registry No.** I, 35796-48-6; Ia, 75701-06-3; Ib, 68193-71-5; Ic, 66219-75-8; Id, 100928-23-2; II, 100928-21-0; IIa, 100928-15-2; IIb, 100928-18-5; III, 100928-22-1; IIIa, 100928-16-3; IIIb, 100928-20-9.

(20) Traylor, T. G.; Stewart, K. J.; Goldberg, M. J. *J. Am. Chem. Soc.* **1984**, *106*, 4445–4454.

Contribution from the Department of Chemistry and Molecular Structure Center, Indiana University, Bloomington, Indiana 47405

# The Tungsten–Tungsten Triple Bond. 12.[1] Bis(1,3-diaryltriazenido)bis(dimethylamido)diethylditungsten (M≡M) Compounds

M. H. Chisholm,* H. T. Chiu, J. C. Huffman, and R. J. Wang

*Received July 31, 1985*

*anti*- and *gauche*-$W_2Et_2(NMe_2)_4$ react with 1,3-diaryltriazenes, ArNNNHAr, where Ar = phenyl (Ph) and *p*-tolyl (*p*-tol), in hydrocarbon solvents to give $W_2Et_2(NMe_2)_2(ArN_3Ar)_2$ compounds in three isomeric forms, A, B, and C. Isomers A and B are formed kinetically from *gauche*- and *anti*-1,2-$W_2Et_2(NMe_2)_4$, respectively. With time, isomer A is converted to isomer B, which reacts further to give an equilibrium mixture of B and C. The isomer B, where Ar = Ph, and isomer C, where Ar = *p*-tol, have been characterized by single-crystal X-ray studies. In both isomers each tungsten atom is coordinated to three nitrogen atoms and one carbon atom in a roughly square-planar manner and united to the other tungsten atom by a W≡W bond. For isomer B (Ar = Ph) the W≡W bond is unbridged, W–W = 2.304 (1) Å, while for C (Ar = *p*-tol) there is a pair of cis-bridging triazenido ligands, W–W = 2.267 (1) Å. On the basis of the observed solid-state structures and NMR studies of the reaction between $W_2Et_2(NMe_2)_4$ and 1,3-diaryltriazenes, a reaction sequence accounting for the kinetic sequence of events is proposed. Crystal data follow for the compounds $W_2Et_2(NMe_2)_2(ArN_3Ar)_2$. For Ar = Ph, at −159 °C: $a$ = 19.504 (5) Å, $b$ = 8.650 (1) Å, $c$ = 19.385 (5) Å, $Z$ = 4, $d_{calcd}$ = 1.841 g cm$^{-3}$, space group *Pbcn*. For Ar = *p*-tol, at −161 °C: $a$ = 12.728 (5) Å, $b$ = 13.990 (7) Å, $c$ = 21.274 (10) Å, $\beta$ = 98.17 (2)°, $d_{calcd}$ = 1.705 g cm$^{-3}$, space group $P2_1/c$.

## Introduction

Following our discovery[2,3] of dinuclear reductive-elimination reactions involving molybdenum, eq 1 and 2 where R = a $\beta$-hydrogen-containing alkyl ligand, we were hopeful that analogous procedures could be used for the synthesis of quadruply bonded (W–W) carbamates and triazenides of tungsten.

$$Mo_2R_2(NMe_2)_4 + 4CO_2 \rightarrow Mo_2(O_2CNMe_2)_4 + \text{alkene} + \text{alkane} \quad (1)$$

$$Mo_2R_2(NMe_2)_4 + 4ArNNNHAr \rightarrow Mo_2(ArN_3Ar)_4 + 4HNMe_2 + \text{alkene} + \text{alkane} \quad (2)$$

However, this did not prove to be the case,[2,4] and the reactions involving $W_2R_2(NMe_2)_4$ compounds have proved much more complex. We describe here our studies of the initial steps of the reaction between $W_2Et_2(NMe_2)_4$ and 1,3-diaryltriazenes, which are well-behaved in yielding isolable compounds of formula $W_2Et_2(NMe_2)_2(ArN_3Ar)_2$, where Ar = Ph and *p*-tol. In a subsequent paper we shall describe how further reactions with triazenes and carbon dioxide proceed.

## Results and Discussion

**Synthesis.** $W_2Et_2(NMe_2)_2(ArN_3Ar)_2$ compounds, I (Ar = Ph) and II (Ar = *p*-tol), can be prepared by mixing $W_2Et_2(NMe_2)_4$ and the 1,3-diaryltriazenes in hydrocarbon solvents at room

(1) Part 11: Ahmed, K. J.; Chisholm, M. H.; Huffman, J. C. *Inorg. Chem.* **1985**, *24*, 3214.
(2) Chisholm, M. H.; Haitko, D. A. *J. Am. Chem. Soc.* **1979**, *101*, 6784.
(3) Chetcuti, M. H.; Chisholm, M. H.; Folting, K.; Haitko, D. A.; Huffman, J. C. *J. Am. Chem. Soc.* **1982**, *104*, 2138.
(4) A general synthesis of ditungsten carboxylates employing a similar strategy was successful: Chisholm, M. H.; Chiu, H. T.; Huffman, J. C. *Polyhedron* **1984**, *3*, 759.

0020-1669/86/1325-1092$01.50/0 

**Table I.** $^1$H NMR Data for the $W_2Et_2(NMe_2)_2(ArNNNAr)_2$ Compounds[a]

| compd | isomer | $CH_aH_bMe$ | $CH_aH_bMe$ | $CH_2Me$ | $NMe_p$ | $NMe_d$ | $C_6H_4Me_a$ | $C_6H_4Me_b$ |
|---|---|---|---|---|---|---|---|---|
| I | A | 2.95 m | *b* | 1.29 t | 3.97 s | 2.03 s | | |
| I | B | 3.08 m | 2.24 m | 1.10 t | 3.92 s | 2.01 s | | |
| I | C | 1.47 m | 1.06 m | 2.60 t | 4.12 s | 2.08 s | | |
| II | A | 2.97 m | *b* | 1.35 t | 4.06 s | 2.10 s | 2.22 s | 2.13 s |
| II | B | 3.13 m | 2.36 m | 1.16 t | 3.99 s | 2.05 s | 2.28 s | 2.08 s |
| II | C | 1.51 m | 1.08 m | 2.66 t | 4.18 s | 1.96 s | 2.18 s | 2.12 s |

[a] All spectra are recorded at 360 MHz in benzene-$d_6$ and reported in ppm relative to $Me_4Si$: p, proximal; d, distal; s, singlet; t, triplet; m, multiplet. [b] Multiplets are not observed due to overlapping with strong $NMe_d$ signals.

temperature according to the stoichiometric reaction shown in eq 3.

$$1,2\text{-}W_2Et_2(NMe_2)_4 + 2ArNNNHAr \rightarrow W_2Et_2(NMe_2)_2(ArN_3Ar)_2 + 2HNMe_2 \quad (3)$$

$$Ar = Ph,\ p\text{-tol}$$

Although a further reaction with more of the 1,3-diaryltriazenes occurs, this is slow relative to the first two substitutions of $NMe_2$ for $ArN_3Ar$ so that the yields in reaction 3 are close to quantitative (by $^1$H NMR spectroscopy) on the basis of the stoichiometry shown. Compounds I and II may be obtained as crystalline solids, dark red or red-brown, by crystallization from toluene/hexane solutions. The crystals so obtained are a mixture of two isomers, B and C, which can be separated by careful crystal picking in the drybox if the crystals are of a suitable size. Examination of the mother liquor reveals the presence of another isomer, particularly at short reaction times: isomer A, in addition to isomers B and C. $HNMe_2$ is removed under vacuum.

**$^1$H NMR Studies.** $^1$H NMR data for each of the three isomers of compounds I and II are given in Table I. All isomers show downfield and upfield resonances assignable to proximal and distal NMe groups. The chemical shift separation between these singlets is roughly 2 ppm due to the magnetic anisotropy of the W≡W bond.[5] The ethyl groups give rise to $ABX_3$ patterns, and there are two types of aromatic rings. In the case of the isomers of II (Ar = *p*-tol), the tolyl methyl resonances appear as two singlets of equal integral intensity for each isomer. Each isomer of I and II has an apparent $C_2$ axis of symmetry.

Of particular interest are the chemical shifts of the methyl groups of the ethyl ligands. In isomers A and B these are in the range 1–1.4 ppm whereas for isomers C of both I and II these methyl signals are downfield at ca. 2.6 ppm. Conversely, the chemical shifts of the diastereotopic methylene protons of the ethyl ligands are upfield in isomers C and downfield in isomers A and B. Though there is no reason to believe that rotations about W–C bonds are frozen out on the NMR time scale, we can correlate these chemical shifts with the average conformational environments of the methylene and methyl protons. In isomers A and B of both I and II, the methyl groups of the ethyl ligand are distal to the W≡W bond while in isomers C the ethyl groups are turned so that the methyl groups lie over (proximal) the M≡M bond. This argument assumes that the magnetic anisotropic of the M≡M bond is the dominant factor influencing the chemical shifts of the ethyl protons and not, for example, the magnetic anisotropy of the aromatic rings of the $ArN_3Ar$ ligands. In view of the solid-state structures of isomers B and C for compounds I and II, respectively, this seems to be justified. However, it is the positioning of the aryl ligands that determines the preferred distal or proximal positioning of the $CH_2Me$ group.

When the reaction between $W_2Et_2(NMe_2)_4$ and PhNNNHPh (2 equiv) in toluene-$d_8$ at −40 °C is monitored by $^1$H NMR spectroscopy, the disappearance of the gauche and anti rotamers of $W_2Et_2(NMe_2)_4$ occur at very similar rates and the formations of isomer A and isomer B are observed. Only a trace of isomer C can be detected initially. No compound of formula $W_2Et_2(NMe_2)_3(PhN_3Ph)$ was detected. Isomers A and B appear to be formed from the gauche and anti rotamers, respectively. Since an equilibrium mixture of *anti*- and *gauche*-$W_2Et_2(NMe_2)_4$ favors the gauche rotamer by ca. 4:1, isomer A predominates initially. After the temperature of the NMR probe is raised to +20 °C, the signals of isomer A decrease as those associated with isomer B increase in intensity. With time, the signals associated with isomer C grow in until after 3 weeks isomer A is negligible but isomers B and C are in the ratio 1:2.

**Scheme I.** Newman Projections Showing the Intermediates in the Reaction between *anti*- and *gauche*-$W_2Et_2(NMe_2)_4$ Molecules and ArNNNHAr, Leading to Isomers (Rotamers) B and A, Respectively, for $W_2Et_2(NMe_2)_2(ArN_3Ar)_2$[a]

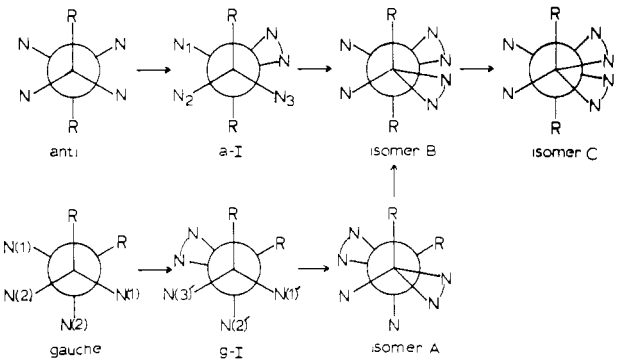


[a] See text for a discussion of the order of $NMe_2$ group substitution.

When a sealed NMR tube of a sample of I (Ar = Ph) containing more than 95% isomer B (a large hand-picked crystal) dissolved in toluene-$d_8$ is followed by $^1$H NMR spectroscopy, the signals due to isomer B decrease as those due to isomer C grow in reaching equilibrium (1:2 for isomer B and isomer C, respectively) in ca. 3 weeks at room temperature. Under analogous conditions, a sample of II (Ar = *p*-tol) containing initially isomer C reaches equilibrium in 1 week with the ratio of the concentrations of isomer B to isomer C being 1:4.

Thus by NMR spectroscopy, the following relationships for the isomers is established: Isomers A and B are formed first in reaction 3. Isomer A then isomerizes to isomer B, which in turn isomerizes to isomer C, setting up an equilibrium between isomers B and C, the position of which is sensitive to the nature of the aryl substituents on the triazenido ligand (eq 4).

$$A \rightarrow B \rightleftharpoons C \quad (4)$$

Since it is clear from the low-temperature NMR study of the reaction between $W_2Et_2(NMe_2)_4$ and PhNNNHPh (2 equiv) that the first introduction of a $PhN_3Ph$ ligand at the ditungsten center is followed rapidly by the second and that the third substitution is much slower, we can most reasonably accommodate our findings by the suggestion that the first and second substitutions occur at different metal centers. Given this assumption, the reaction pathway can be summarized by the compounds shown as Newman projections in Scheme I. The use of Newman projections is appropriate because of the small bite of the $ArN_3Ar$ ligand and the cogging effect of the $NC_2$ blades, which, for electronic reasons, prefer to be aligned along the M–M axis.[7] The ease of substitution

(5) Chisholm, M. H.; Cotton, F. A. *Acc. Chem. Res.* **1978**, *11*, 356.
(6) Chisholm, M. H.; Haitko, D. A.; Huffman, J. C. *J. Am. Chem. Soc.* **1981**, *103*, 4046.
(7) Chetcuti, M. J.; Chisholm, M. H.; Folting, K.; Haitko, D. A.; Huffman, J. C.; Janos, J. *J. Am. Chem. Soc.* **1983**, *105*, 1163.

**Table II.** Fractional Coordinates and Isotropic Thermal Parameters for the $W_2Et_2(NMe_2)_2(PhNNNPh)_2$ Molecule

| atom | $10^4x$ | $10^4y$ | $10^4z$ | $10B_{iso}$, Å$^2$ |
|---|---|---|---|---|
| W(1) | 9947.4 (2) | 2462.4 (4) | 6908.2 (2) | 14 |
| C(2) | 9152 (6) | −1999 (12) | 5960 (6) | 25 |
| C(3) | 8625 (7) | −3049 (14) | 5893 (7) | 31 |
| C(4) | 8120 (6) | −3134 (16) | 6382 (7) | 31 |
| C(5) | 8142 (6) | −2204 (14) | 6947 (6) | 27 |
| C(6) | 8678 (6) | −1204 (14) | 7025 (6) | 26 |
| C(7) | 9196 (5) | −1070 (11) | 6539 (5) | 18 |
| N(8) | 9724 (4) | 2 (9) | 6645 (4) | 16 |
| N(9) | 10301 (4) | −276 (9) | 6325 (4) | 18 |
| N(10) | 10704 (4) | 899 (9) | 6490 (4) | 16 |
| C(11) | 11344 (5) | 1001 (12) | 6168 (5) | 21 |
| C(12) | 11511 (6) | 193 (13) | 5578 (6) | 30 |
| C(13) | 12154 (6) | 401 (15) | 5302 (7) | 33 |
| C(14) | 12630 (6) | 1332 (15) | 5596 (6) | 30 |
| C(15) | 12475 (6) | 2163 (16) | 6167 (6) | 34 |
| C(16) | 11827 (5) | 1983 (14) | 6460 (5) | 25 |
| N(17) | 10362 (4) | 4390 (9) | 6619 (4) | 20 |
| C(18) | 10689 (7) | 5692 (14) | 6955 (7) | 27 |
| C(19) | 10433 (7) | 4560 (16) | 5867 (6) | 32 |
| C(20) | 8867 (5) | 2826 (12) | 6740 (5) | 19 |
| C(21) | 8706 (6) | 2760 (16) | 5964 (6) | 29 |

of a $NMe_2$ group by a triazenido ligand is proposed to be directly related to steric congestion across the M–M bond and specifically to follow the order R–$NMe_2$–$ArN_3Ar$ > R–$NMe_2$–$NMe_2$ > $ArN_3Ar$–$NMe_2$–$NMe_2$ > $NMe_2$–$NMe_2$–$NMe_2$; i.e., the $NMe_2$ ligand bracketed by two $NMe_2$ ligands is the least accessible for attack by a triazene molecule while the $NMe_2$ group bracketed by R and $ArN_3Ar$ is the most accessible. It should also be noted that substitution of an amide ligand involves protonation of the coordinated ligand and does not involve prior dissociation of a $Me_2N^-$ ligand.[8]

In Scheme I we see that the anti rotamer has four equivalent amide ligands, and thus the first substitution is totally arbitrary, yielding a-I. Now there are three different $NMe_2$ groups present at the dinuclear center, and by the above order of substitution, $N_3$, which is bracketed by R and $ArN_3Ar$ ligands, will be most accessible to substitution, yielding isomer B.

The gauche rotamer of $W_2Et_2(NMe_2)_4$ has two types of amide ligands, namely those that are mutually anti, N(1), and those that are anti to the ethyl ligands, N(2). The N(2) dimethylamides are bracketed by two $NMe_2$ ligands and least accessible to attack. Thus, substitution at the gauche rotamer will proceed via the intermediate g-I, which has three different types of amide ligands: N(1)′, N(2)′, and N(3)′. N(1)′ represents the dimethylamide bracketed by R and N(2)′ ligands and will preferentially be substituted to yield isomer A. Note isomer A may isomerize to isomer B by a rotation about the W–W bond, which is hindered by steric factors alone,[9] but a direct conversion of isomer A to isomer C (i.e. without going through isomer B) is not possible.

In conclusion, the substitution of $NMe_2$ groups by $ArN_3Ar$ ligands at the dinuclear center is entirely understandable. The thermodynamic preference for isomer C over isomer B is small because of the nearly balanced opposing factors. The favorable entropy of bridge formation (five-membered rings being favored over four-membered rings) is opposed by steric repulsive interactions since the bridged isomer has a more eclipsed geometry relative to that of the chelate isomer. We find that substitution at the dinuclear center forms initially the chelated triazenido species (these are kinetically favored). The latter finding has a parallel with substitution reactions involving M–M multiple-bonded compounds $M_2X_8^{n-}$ (X = a halide) and their reactions with bidentate phosphines to give either $\alpha$ (chelated) or $\beta$ (bridged) isomers $M_2X_4(L\text{–}L)_2$.[10]

(8) Chisholm, M. H.; Extine, M. W. *J. Am. Chem. Soc.* **1977**, *99*, 792.
(9) Chisholm, M. H.; Folting, K.; Huffman, J. C.; Rothwell, I. P. *Organometallics* **1982**, *1*, 251.
(10) Fraser, I. F.; McVitie, A.; Peacock, R. D. *J. Chem. Res., Synop.* **1984**, 420. Agaskar, P. A.; Cotton, F. A.; Derringer, D. R.; Powell, G. L.; Root, V. R.; Smith, T. J. *Inorg. Chem.* **1985**, *24*, 2786.

**Table III.** Fractional Coordinates and Isotropic Thermal Parameters for the $W_2Et_2(NMe_2)_2((p\text{-tol})_2N_3)_2$ Molecule

| atom | $10^4x$ | $10^4y$ | $10^4z$ | $10B_{iso}$, Å$^2$ |
|---|---|---|---|---|
| W(1) | 8959.6 (4) | 2003.1 (4) | 5941.8 (2) | 19 |
| W(2) | 8684.1 (4) | 3513.4 (4) | 6268.4 (2) | 19 |
| N(3) | 7687 (8) | 2301 (8) | 5127 (5) | 20 |
| N(4) | 7378 (8) | 3163 (8) | 4961 (5) | 20 |
| N(5) | 7749 (9) | 3829 (9) | 5367 (5) | 25 |
| N(6) | 7585 (8) | 1508 (8) | 6334 (5) | 19 |
| N(7) | 6840 (8) | 2085 (8) | 6470 (5) | 21 |
| N(8) | 7046 (8) | 3005 (9) | 6422 (5) | 25 |
| N(9) | 10173 (9) | 1496 (10) | 6487 (5) | 29 |
| N(10) | 10014 (9) | 4215 (9) | 6286 (5) | 27 |
| C(11) | 7341 (9) | 1609 (10) | 4650 (6) | 19 |
| C(12) | 6964 (11) | 1830 (10) | 4016 (7) | 25 |
| C(13) | 6676 (11) | 1139 (11) | 3579 (6) | 27 |
| C(14) | 6701 (10) | 186 (11) | 3748 (6) | 26 |
| C(15) | 7095 (11) | −50 (10) | 4377 (6) | 24 |
| C(16) | 7401 (11) | 654 (11) | 4823 (6) | 24 |
| C(17) | 6385 (12) | −622 (11) | 3272 (7) | 31 |
| C(18) | 7329 (12) | 4763 (10) | 5183 (6) | 26 |
| C(19) | 7903 (11) | 5576 (11) | 5412 (6) | 27 |
| C(20) | 7480 (12) | 6473 (10) | 5289 (7) | 28 |
| C(21) | 6472 (12) | 6606 (11) | 4956 (6) | 29 |
| C(22) | 5951 (13) | 5784 (11) | 4704 (7) | 33 |
| C(23) | 6360 (12) | 4872 (10) | 4814 (6) | 27 |
| C(24) | 5963 (14) | 7568 (11) | 4841 (9) | 41 |
| C(25) | 7318 (11) | 527 (10) | 6410 (6) | 23 |
| C(26) | 8094 (11) | −99 (11) | 6661 (7) | 29 |
| C(27) | 7860 (13) | −1062 (11) | 6745 (7) | 33 |
| C(28) | 6853 (15) | −1390 (11) | 6573 (7) | 35 |
| C(29) | 6072 (12) | −758 (11) | 6300 (7) | 31 |
| C(30) | 6291 (11) | 205 (11) | 6214 (7) | 27 |
| C(31) | 6574 (16) | −2419 (11) | 6669 (9) | 44 |
| C(32) | 6237 (10) | 3589 (10) | 6608 (5) | 21 |
| C(33) | 5317 (10) | 3217 (9) | 6825 (6) | 22 |
| C(34) | 4512 (10) | 3804 (10) | 6946 (6) | 23 |
| C(35) | 4567 (11) | 4799 (11) | 6875 (6) | 26 |
| C(36) | 5489 (10) | 5150 (9) | 6674 (6) | 21 |
| C(37) | 6311 (10) | 4584 (10) | 6548 (6) | 26 |
| C(38) | 3671 (12) | 5466 (12) | 6976 (8) | 34 |
| C(39) | 9815 (11) | 2059 (11) | 5117 (6) | 26 |
| C(40) | 9720 (13) | 2858 (13) | 4614 (7) | 37 |
| C(41) | 8788 (10) | 3478 (10) | 7313 (6) | 22 |
| C(42) | 8541 (12) | 2583 (13) | 7699 (7) | 33 |
| C(43) | 10583 (12) | 565 (12) | 6293 (8) | 37 |
| C(44) | 10891 (12) | 1891 (13) | 7010 (8) | 38 |
| C(45) | 11055 (11) | 3973 (9) | 6137 (7) | 28 |
| C(46) | 10100 (13) | 5117 (12) | 6636 (7) | 38 |

**Table IV.** Selected Bond Distances (Å) and Angles (deg) for the $W_2Et_2(NMe_2)_2(PhNNNPh)_2$ Molecule

| | | | |
|---|---|---|---|
| W(1)–W(1)′ | 2.3036 (9) | N(8)–C(7) | 1.401 (12) |
| W(1)–N(8) | 2.232 (8) | N(9)–N(10) | 1.325 (10) |
| W(1)–N(10) | 2.160 (7) | N(10)–C(11) | 1.397 (12) |
| W(1)–N(17) | 1.936 (8) | N(17)–C(18) | 1.449 (14) |
| W(1)–C(20) | 2.156 (10) | N(17)–C(19) | 1.472 (14) |
| N(8)–N(9) | 1.308 (10) | | |

| | | | |
|---|---|---|---|
| W(1)′–W(1)–N(8) | 104.19 (19) | W(1)–N(8)–N(9) | 96.6 (5) |
| W(1)′–W(1)–N(10) | 108.26 (20) | W(1)–N(8)–C(7) | 143.9 (6) |
| W(1)′–W(1)–N(17) | 104.55 (23) | N(9)–N(8)–C(7) | 116.2 (8) |
| W(1)′–W(1)–C(20) | 103.77 (27) | N(8)–N(9)–N(10) | 104.8 (7) |
| N(8)–W(1)–N(10) | 56.68 (28) | W(1)–N(10)–N(9) | 99.5 (5) |
| N(8)–W(1)–N(17) | 146.8 (3) | W(1)–N(10)–C(11) | 137.6 (6) |
| N(8)–W(1)–C(20) | 85.0 (3) | N(9)–N(10)–C(11) | 118.1 (8) |
| N(10)–W(1)–N(17) | 98.4 (3) | W(1)–N(17)–C(18) | 136.3 (7) |
| N(10)–W(1)–C(20) | 134.6 (3) | W(1)–N(17)–C(19) | 114.4 (7) |
| N(17)–W(1)–C(20) | 103.8 (4) | C(18)–N(17)–C(19) | 109.0 (10) |

**Solid-State and Molecular Structures.** In the solid state the two compounds examined of formula $W_2Et_2(NMe_2)_2(ArN_3Ar)_2$, namely compound I (Ar = Ph) as isomer B and compound II (Ar = *p*-tol) as isomer C, exist as discrete molecules. ORTEP views of I and II are shown in Figures 1 and 2, respectively. Fractional coordinates are listed in Tables II and III, and selected bond distances and bond angles are given in Tables IV and V.

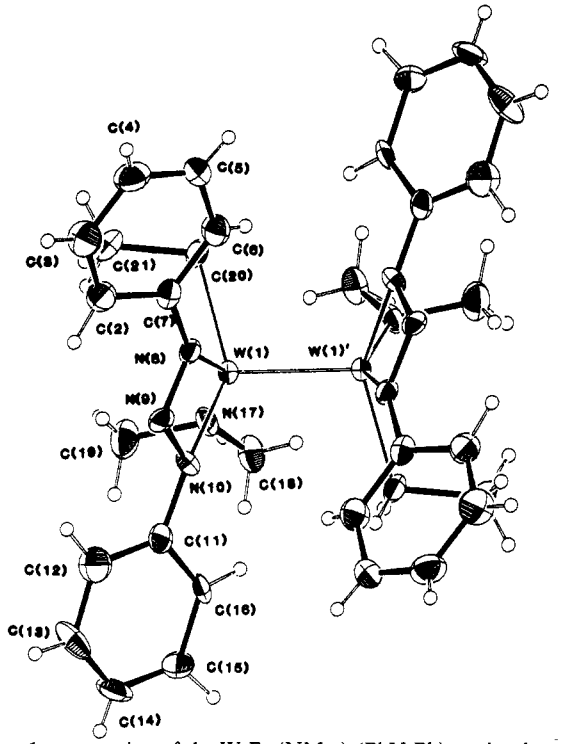


**Figure 1.** ORTEP view of the $W_2Et_2(NMe_2)_2(PhN_3Ph)_2$ molecule, giving the atom number scheme used in the tables.

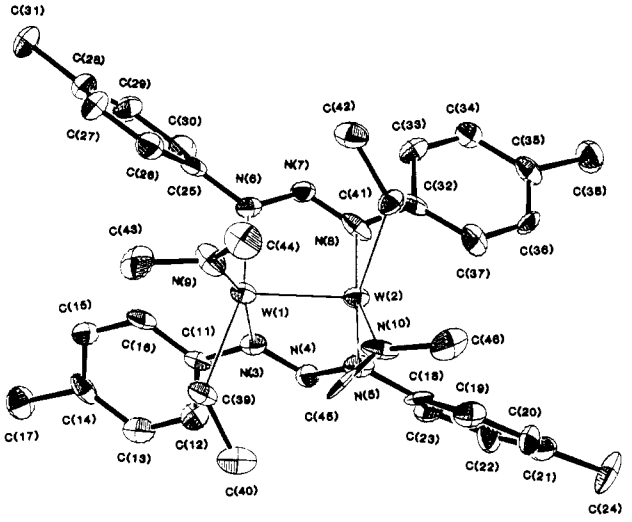


**Figure 2.** ORTEP view of the $W_2Et_2(NMe_2)_2((p\text{-tol})_2N_3)_2$ molecule, giving the atom number scheme used in the tables.

For I, isomer B, the molecule consists of two $WEt(NMe_2)(PhN_3Ph)$ units joined by an unbridged W≡W bond of distance 2.304 (1) Å. The molecule has crystallographically imposed $C_2$ symmetry. The W–N distances associated with the $PhN_3Ph$ ligand, 2.23 (1) and 2.16 (1) Å, reflect the differing trans influences[11] of the $NMe_2$ and Et ligands.

Molecules of II, isomer C, have virtual but not crystallographically imposed $C_2$ symmetry. The molecule is structurally analogous to $Mo_2Et_2(NMe_2)_2((p\text{-tol})_2N_3)_2$,[3] and the W–W distance, 2.267 (1) Å, is very slightly shorter than for I, presumably a consequence of the bridging ligands.

The W–N(amido) and W–C(ethyl) distances for both I and II are comparable to those found previously for compounds containing a central $(M{\equiv}M)^{6+}$ unit (M = Mo or W),[12] and the alignment of the $NC_2$ blades collinear with the W–W bond vector is understandable in terms of $Me_2N$-to-W $\pi$-bonding.[7] Finally, we note the positioning of the methyl groups of the ethyl ligands is proximal in II and distal in I, as inferred from NMR studies described previously, and this conformational preference is determined by the different positioning of the aryl substituents of

**Table V.** Selected Bond Distances (Å) and Bond Angles (deg) for the $W_2Et_2(NMe_2)_2((p\text{-tol})_2N_3)_2$ Molecule

| | | | |
|---|---|---|---|
| W(1)–W(2) | 2.2670 (13) | N(4)–N(5) | 1.312 (15) |
| W(1)–N(3) | 2.237 (10) | N(5)–C(18) | 1.444 (18) |
| W(1)–N(6) | 2.157 (10) | N(6)–N(7) | 1.309 (15) |
| W(1)–N(9) | 1.930 (11) | N(6)–C(25) | 1.428 (17) |
| W(1)–C(39) | 2.195 (12) | N(7)–N(8) | 1.320 (16) |
| W(2)–N(5) | 2.155 (11) | N(8)–C(32) | 1.413 (17) |
| W(2)–N(8) | 2.271 (11) | N(9)–C(43) | 1.483 (20) |
| W(2)–N(10) | 1.951 (10) | N(9)–C(44) | 1.445 (19) |
| W(2)–C(41) | 2.207 (13) | N(10)–C(45) | 1.446 (18) |
| N(3)–N(4) | 1.302 (15) | N(10)–C(46) | 1.461 (20) |
| N(3)–C(11) | 1.426 (17) | | |

| | | | |
|---|---|---|---|
| W(2)–W(1)–N(3) | 86.4 (3) | N(8)–W(2)–N(10) | 165.0 (5) |
| W(2)–W(1)–N(6) | 90.7 (3) | N(8)–W(2)–C(41) | 76.9 (4) |
| W(2)–W(1)–N(9) | 107.7 (4) | N(10)–W(2)–C(41) | 93.7 (5) |
| W(2)–W(1)–C(39) | 109.2 (4) | W(1)–N(3)–N(4) | 122.7 (8) |
| N(3)–W(1)–N(6) | 79.7 (4) | W(1)–N(3)–C(11) | 122.8 (8) |
| N(3)–W(1)–N(9) | 164.5 (4) | W(2)–N(5)–N(4) | 122.8 (9) |
| N(3)–W(1)–C(39) | 76.2 (5) | W(2)–N(5)–C(18) | 124.2 (9) |
| N(6)–W(1)–N(9) | 105.9 (5) | W(1)–N(6)–N(7) | 122.7 (8) |
| N(6)–W(1)–C(39) | 147.4 (5) | W(1)–N(6)–C(25) | 124.8 (8) |
| N(9)–W(1)–C(39) | 92.7 (5) | W(2)–N(8)–N(7) | 120.8 (8) |
| W(1)–W(2)–N(5) | 90.5 (3) | W(2)–N(8)–C(32) | 125.4 (9) |
| W(1)–W(2)–N(8) | 86.4 (3) | W(1)–N(9)–C(43) | 116.0 (9) |
| W(1)–W(2)–N(10) | 107.6 (4) | W(1)–N(9)–C(44) | 133.4 (11) |
| W(1)–W(2)–C(41) | 107.3 (4) | W(2)–N(10)–C(45) | 134.2 (10) |
| N(5)–W(2)–N(8) | 77.9 (4) | W(2)–N(10)–C(46) | 116.5 (9) |
| N(5)–W(2)–N(10) | 106.4 (4) | W(1)–C(39)–C(40) | 125.6 (10) |
| N(5)–W(2)–C(41) | 147.9 (5) | W(2)–C(41)C(42) | 124.2 (9) |

**Table VI.** Summary of Crystal Data[a]

| | I | II |
|---|---|---|
| empirical formula | $W_2C_{32}H_{42}N_8$ | $W_2C_{36}H_{50}N_8$ |
| color of cryst | black | red |
| cryst dimens, mm | 0.08 × 0.08 × 0.11 | 0.15 × 0.15 × 0.11 |
| space group | *Pbcn* | $P2_1/c$ |
| temp, °C | −159 | −161 |
| cell dimens | | |
| *a*, Å | 19.504 (5) | 12.728 (5) |
| *b*, Å | 8.650 (1) | 13.990 (7) |
| *c*, Å | 19.385 (5) | 21.274 (10) |
| $\beta$, deg | | 98.17 (2) |
| *Z* (molecules/cell) | 4 | 4 |
| vol, Å$^3$ | 3270.36 | 3749.65 |
| calcd density, g/cm$^3$ | 1.841 | 1.705 |
| wavelength, Å | 0.710 69 | 0.710 69 |
| mol wt | 906.44 | 962.54 |
| linear abs coeff, cm$^{-1}$ | 72.145 | 62.974 |
| detector to sample dist, cm | 22.5 | 22.5 |
| sample to source dist, cm | 23.5 | 23.5 |
| takeoff angle, deg | 2.0 | 2.0 |
| av $\omega$ scan width at half-height, deg | 0.25 | 0.25 |
| scan speed, deg/min | 4.0 | 5.0 |
| scan width, deg + dispersion | 2.0 | 1.5 |
| individual bkgd, s | 6 | 6 |
| aperture size, mm | 3.0 × 4.0 | 3.0 × 4.0 |
| $2\theta$ range, deg | 6–45 | 6–55 |
| total no. of reflcns collcd | 2612 | 8025 |
| no. of unique intensities | 2143 | 6593 |
| no. with $F > 3.00\sigma(F)$ | 1554 | 5284 |
| $R(F)$ | 0.0345 | 0.0552 |
| $R_w(F)$ | 0.0406 | 0.0545 |
| goodness of fit for the last cycle | 1.020 | 1.251 |
| max $\Delta/\sigma$ for last cycle | 0.05 | 0.05 |

[a] I = $W_2Et_2(NMe_2)_2(PhNNNPh)_2$; II = $W_2Et_2(NMe_2)_2((p\text{-tol})_2N_3)_2$.

(11) Appleton, T. G.; Clark, H. C.; Manzer, L. E. *Coord. Chem. Rev.* **1973**, *10*, 335.
(12) Cotton, F. A.; Walton, R. A. In "Multiple Bonds Between Metal Atoms"; Wiley: New York, 1982.

the triazenido ligands in their bridged and chelated forms.

**Concluding Remarks.** The reaction between 1,2-$W_2Et_2(NMe_2)_4$ and 1,3-diaryltriazenes (2 equiv) has been shown to lead to $W_2Et_2(NMe_2)_2(ArN_3Ar)_2$ compounds. These compounds exist in a mixture of bridged and unbridged forms. There is no evidence for any incipient W---H–C interactions in the ground state, and the compounds are thermally stable at room temperature and not prone to elimination of ethane. This contrasts with the thermally unstable compound $Mo_2Et_2(NMe_2)_2((p\text{-tol})_2N_3)_2$, which is an intermediate in the dinuclear reductive-elimination reaction shown in eq 2.[3] Further studies of the reactions of these $W_2Et_2(NMe_2)_2(ArN_3Ar)_2$ compounds with $CO_2$ and ArNNNHAr are currently under investigation.

## Experimental Section

Care was taken throughout to maintain dry and oxygen-free atmospheres and solvents. $^1H$ NMR spectra were recorded by using a Nicolet NT-360 spectrometer with a low-temperature probe. $W_2Et_2(NMe_2)_4$ was prepared by the published procedure.[6]

**Preparation of $W_2Et_2(NMe_2)_2(PhN_3Ph)_2$.** In a typical preparation, $W_2Et_2(NMe_2)_4$ (0.72 g, 1.2 mmol) and 1,3-diphenyltriazene (0.476 g, 2.42 mmol) were placed in a round-bottom flask and toluene (20 mL) was added. The color of the solution changed from orange to dark red immediately. Then, hexane (15 mL) was added. After the mixture was stored at −30 °C overnight, dark red crystals precipitated. The crystals were distinguished visually under a microscope as a mixture of two isomers; one of them had slightly more brown color (isomer B). Hand separation of the individual isomer from the solid mixture was easily possible when the crystals were of adequate size. A third isomer (A) existed in the filtrate and was identified by NMR spectroscopy. The $^1H$ NMR data of all three isomers are listed in Table I.

Satisfactory elemental analyses were not obtained for bulk crystalline samples, though the data could be fit with ca. one-third of a toluene molecule of crystallization. No toluene or hexane molecules were found in the present X-ray studies, though partial solvent of inclusion was found previously for the related $Mo_2Et_2(NMe_2)_2(Ar_2N_3)_2$ compound.

**Preparation of $W_2Et_2(NMe_2)_2((p\text{-tol})N_3(p\text{-tol}))_2$.** By the same procedure as above with 1,3-di-*p*-tolyltriazene, $W_2Et_2(NMe_2)_4((p\text{-tol})N_3(p\text{-tol}))$ can be obtained. $^1H$ NMR data are listed in Table I.

**Structural Determinations.** General procedures and listings of programs have been reported previously.[13] Crystal data are summarized in Table VI.

**$W_2Et_2(NMe_2)_2(PhN_3Ph)_2$ (I).** A well-formed crystal was transferred to the goniostat by using inert-atmosphere handling techniques. A systematic search of a limited hemisphere of reciprocal space located a set of diffraction maxima of orthorhombic symmetry with extinctions $0kl$ ($k = 2n + 1$), $h0l$ ($l = 2n - 1$), and $hk0$ ($h + k = 2n + 1$), leading to the unique space group *Pbcn*.

The structure solution and refinement proceeded in a normal fashion (direct methods, hydrogens located and refined isotropically). A final difference Fourier was featureless, the largest peak being 0.28 e/Å$^3$. Data were corrected for absorption with minimum and maximum being 0.79 and 0.87, respectively.

**$W_2Et_2(NMe_2)_2((p\text{-tol})_2N_3)_2$ (II).** A suitable fragment was cleaved from a larger crystal and transferred to the goniostat by using standard inert-atmosphere handling techniques. Upon transfer, the sample was cooled to −161 °C for characterization and data collection.

A systematic search of a limited hemisphere of reciprocal space located a set of diffraction maxima, which were indexed as the unique monoclinic space group $P2_1/c$. Data were collected in the usual manner and reduced to a set of intensities and $\sigma$'s. No absorption correction was performed due to the irregular shape and poor definition of the crystalline fragment.

The structure was solved by direct methods (MULTAN78) and Fourier techniques and refined by blocked full-matrix least squares. A difference Fourier phased on the non-hydrogen atoms was able to locate most of the hydrogen atoms in the molecule, and they were included in the final cycles of refinement as idealized, fixed-atom contributors.

A final difference Fourier revealed peaks of 1.0–2.1 e/Å$^3$ in the vicinity of the two tungsten atoms but was otherwise featureless.

**Acknowledgment.** We thank the Office of Naval Research and the Wrubel Computing Center for support.

**Registry No.** IA/IB, 100815-38-1; IC, 100815-39-2; IIA/IIB, 100815-40-5; IIC, 100815-41-6; $W_2Et_2(NMe_2)_4$, 72286-65-8; 1,3-diphenyltriazene, 136-35-6; 1,3-di-*p*-tolyltriazene, 785-86-4.

**Supplementary Material Available:** Tables of anisotropic thermal parameters, VERSORT drawings, complete listings of bond distances and bond angles, and listings of $F_o$ and $F_c$ (35 pages). Ordering information is given on any current masthead page. The complete structure reports are available from the Indiana University Chemical Library in microfiche form only at a cost of $2.50 per report. Request MSC Report No. 84080 for I and 84103 for II.

(13) Chisholm, M. H.; Folting, K.; Huffman, J. C.; Kirkpatrick, C. C. *Inorg. Chem.* **1984**, *23*, 1021.